

INFLUENCE OF COMPATIBILIZER AND SHORT HEMP FIBRES ON THE MECHANICAL, RHEOLOGICAL AND MORPHOLOGICAL PROPERTIES OF RECYCLED POLYETHYLENE TEREPHTHALATE

Maria SÖNMEZ¹, Laurenția ALEXANDRESCU¹, Mihai GEORGESCU¹, Dana Florentina GURĂU¹,
Maria Daniela STELESCU¹, Denisa FICAI^{2*}, Anton FICAI^{2,3}, Roxana TRUȘCĂ², Ioana Lavinia ARDELEAN²,
Doina CONSTANTINESCU⁴, Cristina Elisabeta PELIN⁵, George PELIN⁵, Adriana ȘTEFAN⁵

¹National Research & Development Institute for Textiles and Leather–Division: Leather and Footwear Research Institute, 93
Ion Minulescu St., Bucharest, Romania

²National University of Science and Technology POLITEHNICA Bucharest, Faculty of Applied Chemistry and Material Science;
1-7 Polizu St., Bucharest, Romania

³Academy of Romanian Scientists, Independentei St. 54; Bucharest, Romania

⁴SC MONOFIL S.R.L., 1 Uzinei St., Savinesti, Romania

⁵National Institute for Aerospace Research “Elie Carafoli”, 220 Bd. Iuliu Maniu St., Bucharest, Romania

Received: 09.10.2023

Accepted: 26.04.2024

<https://doi.org/10.24264/lfj.24.2.2>

INFLUENCE OF COMPATIBILIZER AND SHORT HEMP FIBRES ON THE MECHANICAL, RHEOLOGICAL AND MORPHOLOGICAL PROPERTIES OF RECYCLED POLYETHYLENE TEREPHTHALATE

ABSTRACT. The purpose of the paper is to evaluate the influence of maleic anhydride grafted polyethylene (PE-*g*-MA) and untreated/treated hemp fibers on the properties of recycled polyethylene terephthalate (PETr). Blends based on PETr, PETr/PE-*g*-MA (70:30wt%) and composites (67.30:28.85:3.85wt%) based on PETr/PE-*g*-MA/untreated/treated short hemp fibres with 1-5wt% TiO₂ were obtained. Composites were processed using Brabender Plasticorder mixer at 240°C for 7min and pressed to fabricate test specimens. The decoration of hemp fibres with oxide nanoparticles followed by embedding in PETr leads to the fabrication of composites with improved mechanical and thermal properties, this technology being suitable to reuse PET and to develop added-value products.

KEY WORDS: polymer blend or composite, hemp fiber, torque, TiO₂, polyethylene wax, flexural and impact properties

INFLUENȚA COMPATIBILIZATORILOR ȘI A FIBRELOR SCURTE DE CÂNEPĂ ASUPRA PROPRIETĂȚILOR MECANICE, REOLOGICE ȘI MORFOLOGICE ALE TEREFALATULUI DE POLIETILENĂ RECICLAT

REZUMAT. Scopul lucrării este de a evalua influența polietilenei grefate cu anhidridă maleică (PE-*g*-MA) și a fibrelor de cânepă netratate/tratate asupra proprietăților tereftalatului de polietilenă reciclat (PETr). S-au obținut amestecuri pe bază de PETr, PETr/PE-*g*-MA (70:30% în greutate) și compozite (67,30:28,85:3,85% în greutate) pe bază de PETr/PE-*g*-MA/fibre scurte de cânepă netratate/tratate cu 1-5% TiO₂ în greutate. Compozitele au fost prelucrate cu ajutorul malaxorului Brabender Plasticorder la 240°C timp de 7 minute și presate pentru a realiza eșantioane de testare. Decorarea fibrelor de cânepă cu nanoparticule de oxid urmată de încorporarea acestora în PETr duce la fabricarea de compozite cu proprietăți mecanice și termice îmbunătățite, această tehnologie fiind potrivită pentru reutilizarea PET-ului și pentru dezvoltarea de produse cu valoare adăugată.

CUVINTE CHEIE: amestec sau compozit polimeric, fibră de cânepă, moment de torsiune, TiO₂, ceară de polietilenă, proprietăți de încovoiere și de impact

INFLUENCE DES COMPATIBILISANTS ET DES FIBRES COURTES DE CHANVRE SUR LES PROPRIÉTÉS MÉCANIQUES, RHÉOLOGIQUES ET MORPHOLOGIQUES DU POLYÉTHYLÈNE TÉRÉPHTALATE RECYCLÉ

RÉSUMÉ. Le but de l'article est d'évaluer l'influence du polyéthylène greffé à l'anhydride maléique (PE-*g*-MA) et des fibres de chanvre non traitées/traitées sur les propriétés du polyéthylène téréphtalate recyclé (PETr). On a obtenu des mélanges à base de PETr, PETr/PE-*g*-MA (70:30% en poids) et composites (67,30:28,85:3,85% en poids) à base de PETr/PE-*g*-MA/fibres de chanvre courtes non traitées/traitées avec 1-5% du TiO₂ en poids. Les composites ont été traités à l'aide du mélangeur Brabender Plasticorder à 240°C pendant 7 minutes et pressés pour fabriquer des éprouvettes. La décoration des fibres de chanvre avec des nanoparticules d'oxydes suivie de leur incrustation dans du PETr conduit à la fabrication de composites aux propriétés mécaniques et thermiques améliorées, cette technologie étant adaptée pour réutiliser le PET et développer des produits à valeur ajoutée.

MOTS CLÉS : mélange ou composite de polymères, fibre de chanvre, couple de torsion, TiO₂, cire de polyéthylène, propriétés de flexion et d'impact

* Correspondence to: Denisa FICAI, National University of Science and Technology POLITEHNICA Bucharest, Faculty of Applied Chemistry and Material Science; 1-7 Polizu St., Bucharest, Romania, denisaficai@yahoo.ro

INTRODUCTION

In recent decades, a particular emphasis has been placed on recycling plastic materials and the development of new or partially biodegradable composite materials by incorporating compounds from renewable sources (cellulose fibers, chitosan, starch, or other derivatives) [1-3] was found suitable for a sustainable development. The addition of natural ligno-cellulosic fibers in polymers can improve mechanical properties, flexibility and toughness, provided there is good interaction between the phases [4]. The replacement of conventional synthetic fibers (carbon, glass, etc.) with natural fibers (hemp, wood, bamboo, kenaf, flax) in various polymeric composites is a priority and has multiple advantages due to their renewable nature, biodegradability, corrosiveness, recyclability, low energy processing, etc. [5-8]. However, most plant fibers, prior to blending and compounding with various polymeric matrices, are subjected to a pre-drying treatment, which leads to fiber agglomeration due to the formation of oxygen bonds. This fiber agglomeration, together with the percentage of fiber used and the generally high viscosity of the polymers, leads to a poor dispersion, to the formation of the voids and to the reduction of the mechanical properties of the composite. Natural fibers derived from plants contain cellulose as a major structural component [9]. Due to the hydrophilic character of the cellulose and the hydrophobic nature of the thermoplastic matrix, the interaction between the phases is limited [10]. The most commonly used method for improving the polymeric wettability of the fiber surface and, implicitly, the mechanical properties is the treatment with hydroxide (NaOH) [11]. Other treatments focus on physical modification (corona, plasma treatment), chemical modification (esterification-based treatments using silane coupling agents, graft copolymerization, isocyanates, etc.) [12-14]. Hemp fibers are lignocellulose-based fibers and contain ~57-77 wt% cellulose, ~14-22 wt% hemicellulose, ~3.7-13wt% lignin, and waxes in their chemical structure [15].

Particular attention should be paid to the selection of the polymer matrix used for fiber reinforcement as it provides the barrier against

adverse media, protects the surface of the fibers from mechanical abrasion and transfers the loads applied to the fibers [16]. A major limitation in the selection of the matrix used for natural fiber reinforcement is related to the thermal instability of the fibers at temperatures higher than 200°C. For this reason, only those polymers that soften under this temperature, PE, PP, PVC, polystyrene, and thermoactive compounds can be used as matrices [17]. However, some engineering applications require the development and use of composite materials based on high temperature melting thermoplastics reinforced with natural fibers. Obtaining such materials is difficult because engineering thermoplastics have a melting point > 200°C, above the degradation temperature of natural fibers [18, 19]. In addition to these temperature differences, fiber reinforcement is influenced by other factors: fiber type, configuration, composition, length, harvest season, post-harvest treatment, humidity, etc. [20, 21]. These factors, together with thermal stability, drastically influence the properties of the composites during the development process, thus limiting their use in various applications [22]. Thus, for the obtaining of high temperature thermoplastic composites, it is necessary to modify the surface of the fiber in order to avoid degradation during processing.

One of the engineering thermoplastic polymers, widely used for the manufacture of beverage bottles, is polyethylene terephthalate (PET). Due to the short usage period and the very high annual consumption, over millions of tons, it makes recycling a problem both ecologically and economically [23]. Recycling is the most cost-effective method for removing PET waste, thus offering cheaper material than virgin. Physical recycling by reprocessing PET in the melt is considered the simplest method because it requires minimal investment due to the high volume and availability of PET, can be achieved on ordinary processing equipment and is also environmentally friendly. However, during recycling, PET undergoes a number of chemical, mechanical, thermal and oxidative degradations that lead to lower intrinsic viscosity / molecular mass and implicitly lower thermal and mechanical properties [24]. From

this point of view, many studies have focused on blending PET with other polymers: polycarbonate [25], HDPE [26], polypropylene [27-29], polyvinyl chloride (PVC) [30]. Unfortunately, these polymers are incompatible with PET and require the use of an interface compatibilizer, the most used being maleic anhydride graft polymers. Other methods have focused on the use of compounds known as chain extenders to improve viscosity and limit PETr degradation processes. The most commonly used is the multifunctional epoxy-based oligomeric chain extender (Joncryl), mainly added at the start of / during PET melt processing [31, 32]. Another study focused on the addition of styrene and ethylene / butylene (SEBS) triblock copolymer as impact modifier, and PE-g-MA as interface compatibilizer, in the blend containing recycled polymers (HDPE and PET). 4,4'-methylenebis (phenyl isocyanate) (MDI) was investigated as a chain extender. The chain extension reaction of the carboxyl or hydroxyl groups of PETr with the isocyanate groups in MDI and the reaction of the hydroxyl groups of R-PET with anhydride groups of PE-g-MA was observed. The study found that the reaction between anhydride and hydroxyl groups led to the formation of esters, and that urethane linkage is formed between the hydroxyl and isocyanate groups. Interactions between the carboxyl group and the isocyanate lead to the formation of amide linkages. The flexural strength and modulus obtained with the PETr / HDPEr / SEBS / PE-g-MA / MDI blend (70: 30: 5: 2: 0.5) was 23.2MPa, 0.7 GPa, respectively. For recycled HDPE (27.1MPa, 0.64 GPa), and for PETr (83.3 MPa and 2.83 GPa). The impact resistance in the PETr / HDPEr / SEBS / PE-g-MA / MDI blends was 12.16 KJ/m², and the one obtained for HDPEr (13.35 KJ/m²) and PETr (3.89 KJ/m²) [33]. Another study focused on the addition of hemp fibers (1%, 5%, 10%, 15%, and 20%) to limit thermal degradation of PET. The mixtures were processed in a torque batch mixer at 240, 250 and 260 °C. Heavy thermal degradation of hemp fibers was influenced by the amount and processing time that were higher [19]. Pereira *et al.* [34] studied the effect of the addition of poly(ethylene methacrylate) (EMA) and cotton linter (CL) on the properties of recycled

poly(ethylene terephthalate) (PETr). To improve compatibility between EMA and PETr, ethylene / methyl acrylate / glycidyl methacrylate terpolymer (EMAGMA) and maleic anhydride grafted polyethylene (PE-g-MA) were used. The rheological results showed that the torque value measured after 30 minutes, in the case of the non-compatibilized mixture – PETr / EMA (ratio 70:30) was 1.6 Nm versus 1.0 Nm obtained for PETr. The addition of 1% CL in the PETr / EMA / CL mixture decreases the torque value to 0.9 Nm, indicating that viscosity decreases and, implicitly, degradation phenomena are favored. In the case of PETr / EMA / EMA-GMA / CL and PETr / EMA / PE-g-MA / CL mixtures containing compatibilizer, the torque values increase to 1.2 and 1.3 Nm, however, to a rather low extent relative to PETr. The tensile strength obtained in these blends is, however, inferior to PETr. İzgi *et al.* [35] obtained different mixtures based on *Cynara scolymus* / polyethylene terephthalate fibers (72/25, respectively 25/75%) and investigated their influence on the mechanical properties. The tensile strength of the mixture (75/25% *Cynara scolymus* / PET) was 11.84 and for the mixture (25/75% *Cynara Scolymus* / PET) of 9.87 N/mm² relative to PET (3.77 N/mm²). The most common methods for obtaining lingo-cellulosic fiber reinforced composites are: vacuum-infusion process [36], hand-layup technique [37], pultrusion, melt mixing, etc. [38, 39].

The purpose of this paper is to evaluate the influence of the addition of polypropylene grafted with maleic anhydride and untreated / treated hemp fibers on PETr's physico-mechanical, thermal, rheological and morphological properties.

MATERIAL AND METHODS

Materials

Polyethylene terephthalate in the form of flakes was obtained by the industrial partner SC MONOFIL SRL by recycling of municipal waste bottles using a knife mill; Maleic anhydride modified mLLDPE (PE-g-MA) - Bondyram TL4109E, MFI 190°C/2.16 Kg: 2, density g/cm³: 0.905, melting point °C/F: 117/243, Vicat softening point °C/F: 85/185, maleic anhydride

%; high, from Polyram, Israel; 2.2; hemp fibers of 3-5 mm; Isopropanol – molecular weight: 60.10, assay $\geq 99.7\%$, Sigma-Aldrich; Titanium(IV) isopropoxide – molecular weight : 284.22, assay: $\geq 97.0\%$, density: 0.96 g/mL at 20 °C(lit.), acquired Sigma Aldrich; Non polar polyethylene wax – Deurex E11K, drop point, °C: 110-120, viscosity, mPas ≤ 80 , density, g/cm³: 0.94-0.96, acquired from Deurex AG, Germany.

Obtaining Composites

In order to obtain composite materials, the hemp fibres were functionalized according to the following two routes:

Route 1 – The first synthesis route involves the spraying of the titanium isopropoxide (1 and 5%wt in anhydrous isopropanol) onto the surface of the cotton fibers, followed by precipitation of the TiO₂ by spraying water, the precipitation of the TiO₂ nanoparticles happening very fast.

Route 2 – The second synthesis route consists in treating the cotton fibers with water followed by the spraying of titanium isopropoxide (1 and 5%wt in anhydrous isopropanol) onto the surface of the wet cotton fibers while TiO₂ are obtained.

In both cases, the functionalized fibres were dried in vacuum oven at 50 °C before compounding with the polymeric blends.

All blends/ composites were obtained in the presence of compatibilizer – PE-*g*-MA, introduced in an amount of 30wt% (relative to the amount of PETr) and in the presence of 4 wt% treated/untreated natural fibers (relative to the total amount of PETr/PE-*g*-MA). Formulations presented in Table 1, were processed in a 350 E Brabender mixer, with maximum mixing capacity of 370 cm³. Prior to processing, PETr flakes were dried in a hot air oven for 24 hours at 150°C. Dried PETr flakes were used to obtain the mixture (P1) or the composites (P11-P14). When adding

untreated/treated natural fibers to the blend, due to the density difference between PETr and fibers, PE-based wax is used. In these blends, dry and warm PETr flakes were initially mixed with 10 wt% PE-based wax (relative to the amount of fibers) in order to adhere to and disperse the fibers as homogeneously as possible on the surface of the PETr granules. All formulations presented in Table 1, were processed in the Brabender mixer, under similar conditions of temperature, screws speed, mixing time and amount, to limit experimental errors as much as possible. It is important to mention that even if both routes of hemp functionalization involved two concentrations (1 and 5% wt of titanium isopropoxide in anhydrous isopropanol) only two of these functionalized fibres will be presented because the other two composites led to low mechanical properties. During the mixing, the influence of compatibilizer and treated/untreated natural fibers on torque and temperature was monitored, depending on the mixing time. The temperature set for all samples on the three Brabender mixing zones was 240°C, a total mixing time of 7 minutes (of which 1 minute at 30 rpm and 6 minutes at 110 rpm), in order to obtain a more homogeneous dispersion of the compatibility agent and hemp fibers in the molten PETr mass. From the processed blends, physico-mechanical test specimens were obtained in an electric heated press, by the compression method, using the following parameters: the temperature of the plates – 243°C; pre-heating time – 3 minutes; pressing time – 4 minutes, cooling – 10 minutes, force – 300 kN. The specimens for physical, mechanical and thermal properties (flexural, elongation, modulus, Charpy shock, density, hardness, Vicat) had the following dimensions: length – 80 mm, width – 10 mm and thickness – 4 mm. Subsequently, fractured specimens after Charpy shock resistance determination were subjected to morpho-structural determinations (SEM, FTIR microscopy).

Table 1: Formulations of processed blends/composites, wt%

Raw materials/ Sample symbol	PETr	P1	P11	P12	P13	P14
PETr flakes	100	70	70	70	70	70
PE-g-MA	-	30	30	30	30	30
Hemp fibers	-	-	4	-	-	-
Hemp fibers immersed in isopropanol	-	-	-	4	-	-
Hemp fibers functionalized with 1% titanium isopropoxide, according to route 1*	-	-	-	-	4	-
Hemp fibers functionalized with 5% titanium isopropoxide, according to route 2**	-	-	-	-	-	4
PE-based wax	-	-	10	10	10	10

* the composites obtained using hemp fibres functionalized with 5%wt titanium isopropoxide in anhydrous isopropanol, according to route 1, exhibited low mechanical properties and are not presented in this manuscript

* the composites obtained using hemp fibres functionalized with 1%wt titanium isopropoxide in anhydrous isopropanol, according to route 2, exhibited low mechanical properties and are not presented in this manuscript.

Tests and Analysis

Torque rheometry – mixtures / composites were processed in a Brabender type 350E mixer equipped with a temperature measurement sensor in the mixing chamber. It also features temperature, torque, and speed measurement and control elements. These parameters can be controlled / set up and recorded in real-time by specialized software, with the possibility of data interpretation and statistical analysis, at various points of interest.

The 3-point **flexural tests** were performed according to the SR EN 178 standard with a minimum of 6 specimens, at a speed of 2 mm/min, at conventional deflection (1.5 x specimen thickness) and the distance between supports of 16 x specimen thickness. Flexural strength, elasticity modulus, and flexural elongation were determined.

The impact resistance of the mixtures / composites was determined using INSTRON (CEAST 9050) hammer-pendulum equipment. Charpy resistance was determined on notch specimens, using a hammer with a maximum energy of 2J. The determinations were carried out according to ISO 179, method A, the Charpy test type, at a 150° angle, support span 62, using a number of 10 specimens with a length of 80 mm and a thickness of 4 mm.

Density, g/cm³ – mixtures / composites were determined according to SR ISO 2781: 2010.

Hardness, °ShD was determined according to the SR ISO 7619-1:2011 standard.

FTIR microscopy and FTIR spectra were performed to determine the individual components found in the sample (at specific

wavelengths) and to determine the degree of compatibility between the phases. The images were obtained with a Thermo iN10 MX microscope operated in reflection mode.

Scanning Electron Microscopy (SEM) was used to study the morphology of untreated / treated hemp fiber surface, deposition rate, TiO₂ particle size measurement, fiber distribution in PETr mass, interface between fiber / polymer matrix and type of mechanism involved in composite failure. SEM images were recorded on a Quanta Inspect F scanning electron microscope (FEI-Philips, Hillsboro, OR, USA) with a field emission gun at an accelerating voltage of 30 kV with a resolution of 1.2 nm.

Vicat Softening temperature was determined according to the ISO 306 standard.

RESULTS AND DISCUSSION

Torque/Temperature/Time Analysis

Figure 1 and Figure 2 show temperature and torque versus time registered by the Brabender laboratory mixer for PETr, PETr/PE-g-MA (P1) and PETr/PE-g-MA composites reinforced with untreated / treated short natural fibers (P11-P14), processed in similar conditions (time, temperature, screw speed, etc.) to limit the experimental errors. As can be seen, when PETr is being processed, due to its high hardness, torque increases to 222 Nm in just 4 seconds at the time of loading, then drops to about 110 Nm after a 60-second mixing time. Upon increasing the mixing speed to 110 rpm, the torque increases to about 140 Nm, then decreases progressively to 30 and

24.8 Nm in the 224 and 416 seconds respectively. A sudden rise in temperature at 258°C is observed, in the range of 4-224 seconds, after which the temperature remains constant until the end, Figure 2. This clearly demonstrates that PETr is completely melted in 224 seconds, also taking into account that the torque remains constant. At first glance, it can be deduced that the PETr melt processability is excellent, taking into account the torque, and temperature, during the last processing step. However, in the last stage of processing, the torque drops by approximately 17%, which could be attributed to PETr degradation (decrease in molecular weight, reflected in decreased intrinsic viscosity). It is known that the viscosity reduction is directly proportional to torque. These observations are in very good

agreement with studies conducted by other researchers [32, 40]. For PETr, mainly due to the higher hardness than the other mixtures (P1 or P11-P14), the initial torque corresponds to the friction dissipation, and plastic deformation. The torque is directly proportional to the rate of mechanical energy dissipation inside Brabender's mixing chamber. In this way, the mechanical energy is dissipated in the form of heat and leads to the temperature rise, resulting in the melting of the PETr matrix. Instead, if PETr and lower hardness polymers are used, the initial torque moment decreases because the viscous energy dissipation mechanism is different from the dissipation mechanism which takes place between solid particles of high hardness [1].

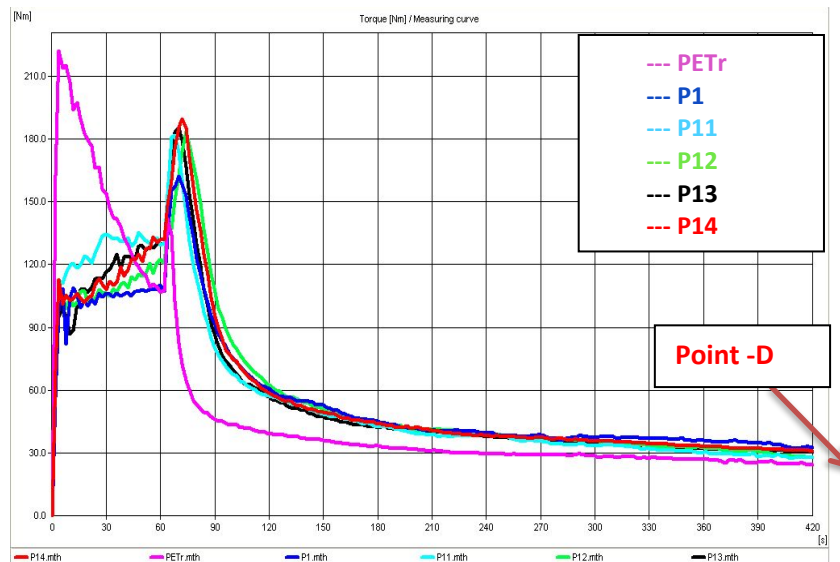


Figure 1. Torque versus time for PETr, P1, and P11-P14 samples

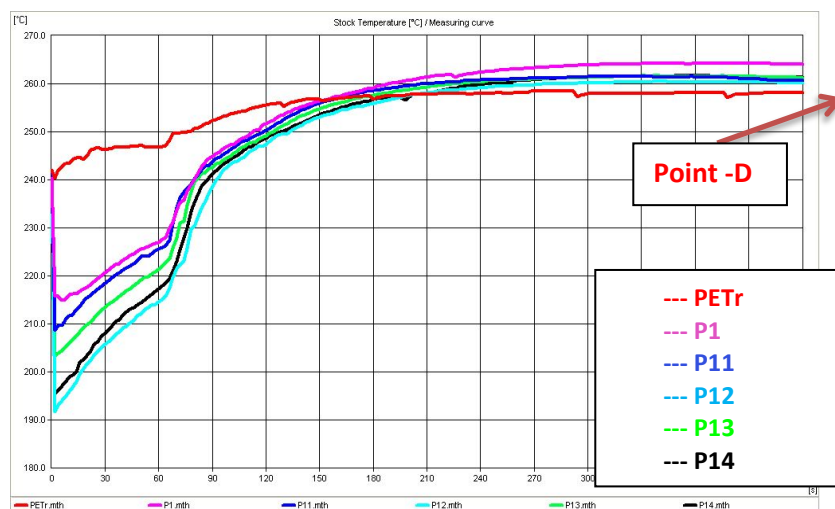


Figure 2. Temperature versus processing time for PETr, P1 and P11-P14 samples

Therefore, in the case of the mixtures P1 and P11-P14, a decrease in the initial torque as well as the temperature, as compared to the values obtained in PETr, is observed. In order to be able to demonstrate that the addition of PE-g-MA improves the torque value and implicitly the viscosity, due to the limitation of PETr degradation

processes, a detailed analysis of point D was performed. Evaluation of point D, recorded at the end of the mix (7 minutes), provides very important information regarding the influence of PE-g-MA and untreated / treated fibers on the torque value. The values obtained for all samples are presented in Table 2.

Table 2: Statistical Evaluation – Point: D of PETr, P1 and P11-P14 samples

Tests	Time [s]	Torque [41]	St. temp. [°C]	Speed [1/min]	Energy [kJ]
PETr	416	24.8	258.2	110.0	170.4
P1	410	32.5	264.2	110.0	223.3
P11	416	28.0	260.8	110.0	215.8
P12	416	28.2	260.3	110.0	228.4
P13	416	30.6	261.4	110.0	219.3
P14	416	31.3	261.4	110.0	227.9

Analyzing the results presented in Table 2, for PETr, it is found that the torque and energy values are only 24.8 Nm and 170.4 kJ at the end of the mixing process. That demonstrates the viscosity of the PETr mixture is low. Instead, mixtures containing PE-g-MA and / or untreated / treated fibers with varying percentages of TiO₂ show improved torque values by 30% (P1), 12.9% (P11), 13.7% (P12) 23% (P13), and 26% (P14) compared to PETr. Also, for all mixtures, there is a substantial increase in temperature, and energy required for mixing, compared with PETr.

Although the torque value is improved for samples P1 and P11-P14, compared to PETr, it should be noted that there is a fairly substantial influence of the addition of unfunctionalized / functionalised fibers. For P11 and P12 samples containing non-functional fibers and immersed only in isopropanol, the torque value decreases to 28 and 28.2, respectively, compared to 32.5 for P1 (PETr / 30% PE-g-MA). This decrease can be attributed to the fact, that in these cases, the interaction between the OH- (fiber) group, the PETr terminal groups and the PE-g-MA anhydride group is weak, such as Van der Waals, hydrogen. These bonds do not have the same strength as the covalent bond and as such they fail to maintain viscosity in the same parameters as the P1 sample (where the reaction is of a chemical nature, between the

terminal PETr group and the PE-g-MA anhydride group). In contrast, for samples P13 and P14, the torque value is very close to that obtained with the P1 sample due to the formation of strong chemical bonds / strong interactions between the of TiO₂ surface-coated fibers, the anhydride group of PE-g-MA, and the terminal groups from PETr (-COOH or OH). It is also noted that as the amount of TiO₂ deposited on the surface of the fibers is higher, the viscosity is more pronounced. Pereira *et al.* [34], Zimmerman and Zattera [42] note that the presence of anhydride-terminal coupling agents promotes the formation of hydrogen or covalent chemical bonds between polymeric and fiber phases, leading to higher molar mass. Moreover, in the SEM one can see a very good compatibility between the phases, especially the mixture (P1) and the P13 and P14 composites, which demonstrates the good interaction between the components in the system, similar to the observations made by Chiu and Hsiao [27].

Physico-Mechanical Determinations

Hardness and Density

The hardness values obtained for the processed blends are presented in Figure 3. It can be seen that the highest hardness of 81 °Sh D is presented by PETr, which also demonstrates the high values of the initial

torque moment recorded in the Brabender mixing chamber. For sample P1, due to the addition of a high 30% PE-g-MA, the hardness value is substantially reduced to 75 °Sh D. In the case of P11 and P12 mixtures containing untreated fibers, the hardness values did not change significantly, relative to sample P1. The samples P13 and P14, however, show hardness values increased proportionally with increasing

of the TiO₂ percentage, present on the fiber surface, up to 76 and 78 °Sh D respectively. This was to be expected because the addition of inorganic particles in the polymer mass increases the hardness and substantially improves the mechanical properties provided it is homogeneously dispersed in the polymer mass and there is a good interaction with the components in the system.

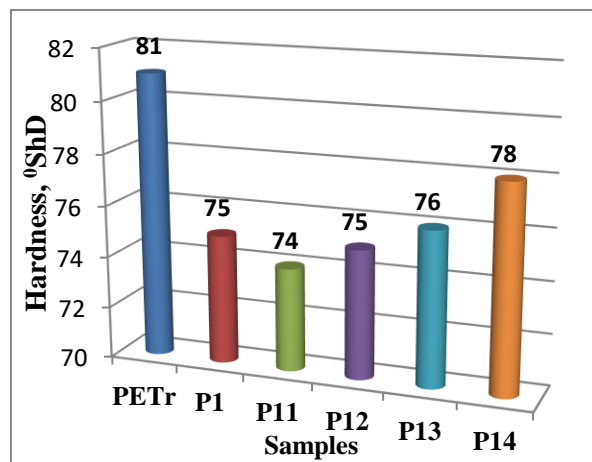


Figure 3. Hardness values obtained for PETr, P1 and P11-P14 samples

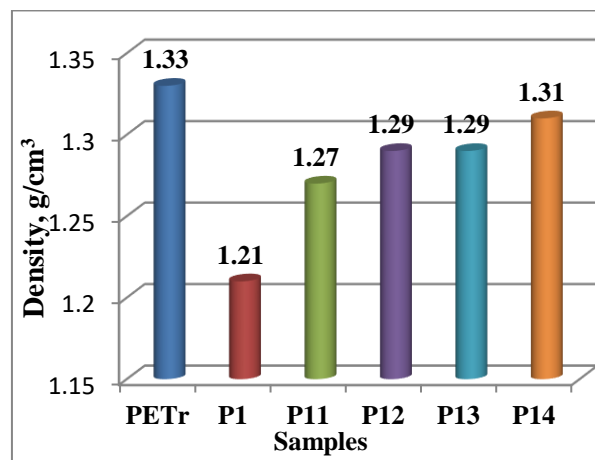


Figure 4. Density values obtained for processed samples

As can be seen from Figure 4, the density of all mixtures decreases relative to the value obtained on PETr. The lowest density value is obtained for the P1 mixture followed by the P12 mixture. If TiO₂ treated fibers are added, a slight increase in density is observed. Density is an important parameter in many areas (and especially automotive, aeronautics, etc.), where materials with improved mechanical properties, environmentally friendly but also with low density are increasingly required

(taking into account economic considerations, and in particular fuel economy).

Flexural Properties

The flexural properties of the blends / composites were determined using a 3-point flexural test. All blends / composites subjected to this type of test were obtained under similar conditions of temperature, time, pressure, etc. (in the Brabender mixer followed by obtaining the test specimens in an electric heated press)

in order to be able to accurately determine the influence of compatibilizer addition and untreated / treated natural fibers on PETr properties. The flexural strength for PETr shows the lowest value – only 17.72 MPa, of all the tested mixtures, which demonstrates that repeated cycles of heating / cooling at high temperatures / pressures lead to massive PETr degradation. The PETr flexural modulus, and

elongation are significantly lower than the values obtained for PE-*g*-MA and / or fiber mixtures. Moreover, visually, PETr specimens obtained showed very high, both hardness and friability. It is also important to mention that PETr flakes used to obtain blends were not pure because they contained materials from caps, especially polypropylene.

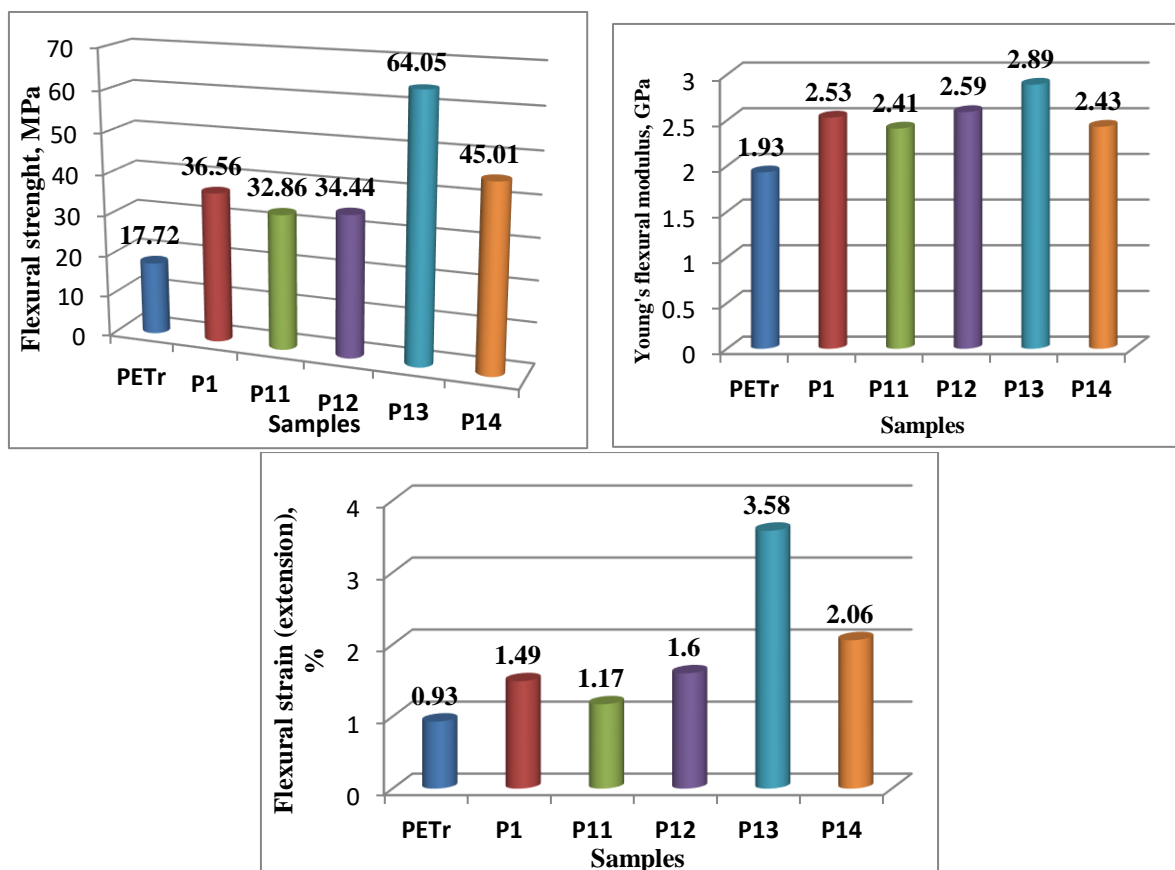


Figure 5. Flexural properties (resistance, modulus, and elongation) of PETr, P1 and P11-P14 samples

In the case of the P1 mixture, it is observed that the addition of PE-*g*-MA in PETr significantly improves bending properties. It is noted that flexural strength increases by 106% relative to the value obtained in the case of PETr. Moreover, Young's modulus and elongation improved by 31 and 187% respectively compared to PETr. These results demonstrate that the addition of PE-*g*-MA is beneficial, being able to greatly limit the PETr degradation due to the bonds formed between the PE-*g*-MA anhydride group and the PETr terminal groups, thus increasing the molecular mass of PETr and implicitly the bending properties. Furthermore, PE-*g*-MA used in

blends has a high viscosity due to the high percentage of maleic anhydride – 30% – grafted on the PE surface. Increasing the number of anhydrous groups allows the formation of a high number of chemical bonds with the existing PETr groups, bonds that lead to an increase in molecular weight, similar to the observations made by Pereira *et al.* [34]. Visually, it can be seen that the addition of PE-*g*-MA significantly improves PETr friability. The obtained specimens were also subjected to bending by hand, observing a very good deformability compared to the PETr specimens that were instantly breaking. Moreover, the films obtained from this mixture could be

subjected to a rather high number of flexions, until the cracks appeared/material failure.

In the case of the P11 and P12 mixtures, it is observed that bending properties increase relative to PETr but are inferior to those obtained in the case of P1 mixture. Thus, flexural strength decreases by 10 and 3% in the case of P1 and P12 mixtures relative to P1. Young's modulus decreases by 4.7% for P11, but increases by 2% for P12 as compared to P1. Similar behavior is observed in the case of the elongation values; for P11 mixture, the elongation decreases by 21.5%, but increases by 7% in the case of the P12 mixture. As noticed, the addition of untreated natural fibers or just immersed in alcohol reduces flexural strength, probably due to slight agglomerations in PETr mass and limited compatibility between phases.

Very good flexural strength values were obtained, however, in the case of adding fibers whose surface was treated with 1% and 5% TiO₂ respectively, samples P13 and P14. As it can be seen, the flexural strength increases by 75 and 23% respectively for samples P13 and P14 relative to sample P1. Young's modulus improves by 23% for P13 but decreases by 4% for P14 composite compared to P1. Bending elongation shows a substantial increase of 140 and 38% for P13 and P14 mixtures compared to those obtained for P1. The reduced elongation of P14 composite compared to P13 may be attributed to the 2°ShD hardness increase. The results show a significant improvement in PETr bending properties, both by the addition of PE-g-MA (improves the ductility and phase compatibility) and the addition of treated fibers. Furthermore, a very high influence of the treatment applied to the surface of the fibers on the bending properties is noticed, because the presence of the TiO₂ groups improves the interactions with the polymeric components in the system, limits to a higher extent the agglomeration of the fibers and protects their surface against thermal degradation, due to high processing temperatures.

Impact Resistance

Impact resistance is a very important property of composite materials because it

provides information on the maximum energy to which a material may be subjected before it breaks. In general, polyesters both recycled and virgin have low impact resistance, mainly due to their very high hardness. To improve their strength, numerous research studies have focused on the addition of flexible (especially elastomeric) chains to improve ductility. The mixtures / materials obtained in this work, Figure 6, show very different shock resistance values and are strongly influenced by the composition. All Charpy impact resistance determinations were carried out in similar conditions using a number of 10 notch specimens and a pendulum with 2J energy. In PETr, a very low shock resistance of only 1.02 kJ/m² is observed, due to, in particular, very high friability and thermal degradation that occurred during processing. A very pronounced improvement in resistance of up to 7.09 kJ/m² was observed in the P1 mixture, which demonstrates that the addition of PE-g-MA, due to its very good compatibility with PETr and its elasticity, reduces friability and absorb applied mechanical energy. In the case of P11 and P12 mixtures, the shock resistance is less than just 4.48 and 6.7 kJ/m² respectively, compared to those obtained with the P1 mixture due to poor interactions / adhesions between the fibers and the polymers in the system, these findings are supported by the SEM microscopy. In these cases, the failure of the material occurs predominantly by pulling out the fibers. Generally, this is the main mechanism for failure of fiber-reinforced materials, in the case of impact assessments, phenomenon also observed by other authors [37, 43]. Substantial increases in impact strength values of 13.78-14.67 kJ/m² were obtained for P13 and P14 mixtures containing titanate-treated fibers. The SEM images obtained confirm the deposition of a generous polymer layer on the surface of the fibers and a very good insertion of these in the PETr mass. In these cases, could not be seen areas where the fibers were pulled or fractured from the matrix. Therefore, the addition of an optimal amount of PE-g-MA has the ability to improve Charpy impact because it improves PETr ductility by acting as a stress transfer agent, limiting phase debonding and allowing for

strong interactions between components [44]. It is known that, the higher the interfacial

adhesion between fibers and matrices, the higher the impact resistance [26, 37, 45].

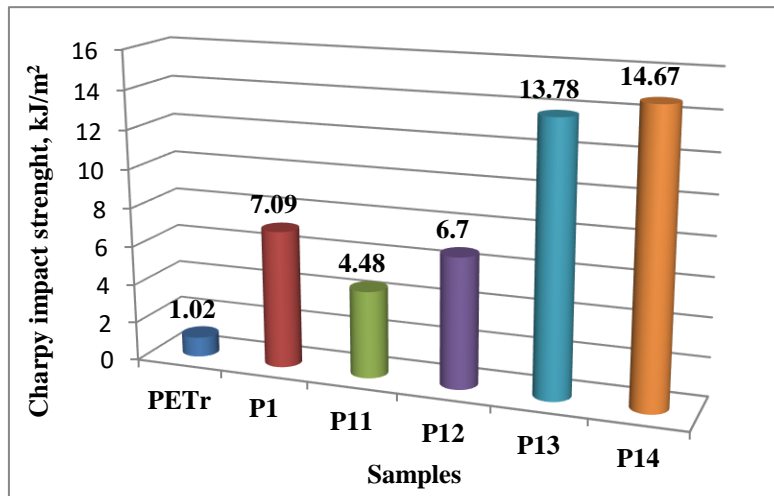


Figure 6. Impact resistance for PETr, P1 and P11-P14 samples

Thermal Analysis

Vicat Softening Point

The Vicat temperature reflects the softening point and is an important parameter with regard to the maximum temperature at which the material can be used in a given application. Table 3 presents the Vicat temperatures obtained for the PETr, P1 and P11-P14 mixtures. It can be seen that PETr has the highest softening point, 210°C. The introduction of PE-g-MA into the PETr (P1) mixture decreases the Vicat temperature by

almost 85°C. This was to be expected because PE-g-MA has a softening point of about 85°C, much lower than PETr. If TiO₂-functionalised hemp fibers are used in 5% (P14) and 1% (P13), the Vicat temperature increases by approximately 7 to 5°C compared to P1 but is maintained at low values compared with PETr. These results clearly indicate that PE-g-MA greatly decreases the thermal properties, and in applications requiring high temperatures, it is necessary to compensate for these losses, either by the addition of stable thermal oxides in higher quantities or by the addition of synthetic fibers (glass, carbon, etc.).

Table 3: The softening temperature of the processed mixtures

Determination/Samples	PETr	P1	P11	P12	P13	P14
Vicat softening point, °C	210	125	127	129	130	132
Softening interval, °C	230-240	140-150	135-145	140-150	142-152	145-155

Morpho-Structural Characterisations

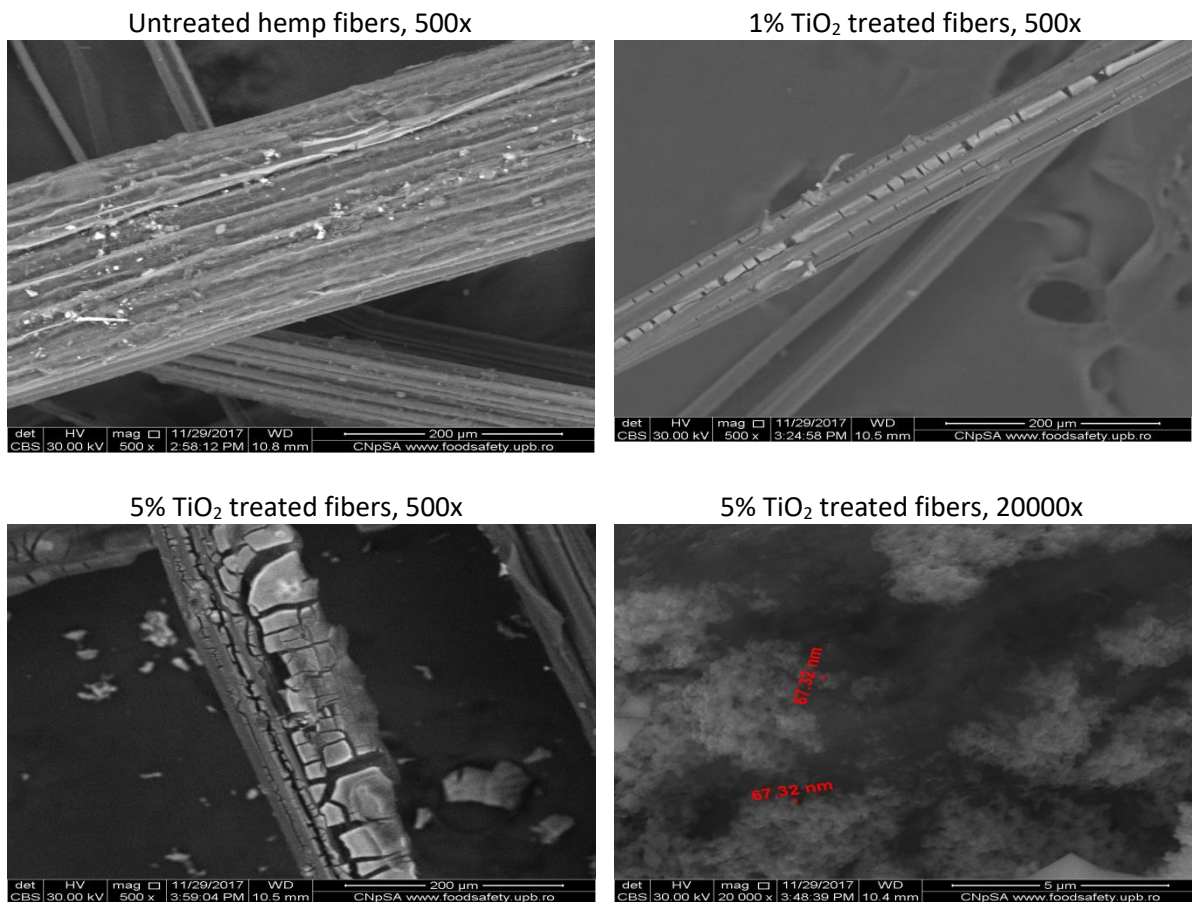
Scanning Electron Microscopy and EDS Spectra

Scanning electron microscopy was used to study the morphology of untreated / treated hemp fiber surface, TiO₂ particle size measurement, PETr mass distribution, interface between the fiber / polymer matrix, and the type of mechanism involved in composite failure. In Figure 7, SEM images obtained on untreated / treated hemp fibers with different amounts of TiO₂ are shown. For

the images recorded on non-functional hemp fibers, fine layers with the non-cellulosic structure deposited on the surface (wax, pectin) and impurities can be seen. In the case of 1% TiO₂ modified fibers, a uniform deposition of the powder on the fiber surface is observed. Also, for fibers treated with 5% titanium isopropoxide, the thickness of the deposited layer is much higher compared to that obtained with 1% titanium isopropoxide. In this case, a relatively uniform deposition of TiO₂ on the surface of the fiber is observed,

which shows that the chosen modification method is suitable. At 20000x magnification, it is observed that the TiO₂ particle shape is

spherical, and the size falls within the nanometer range.

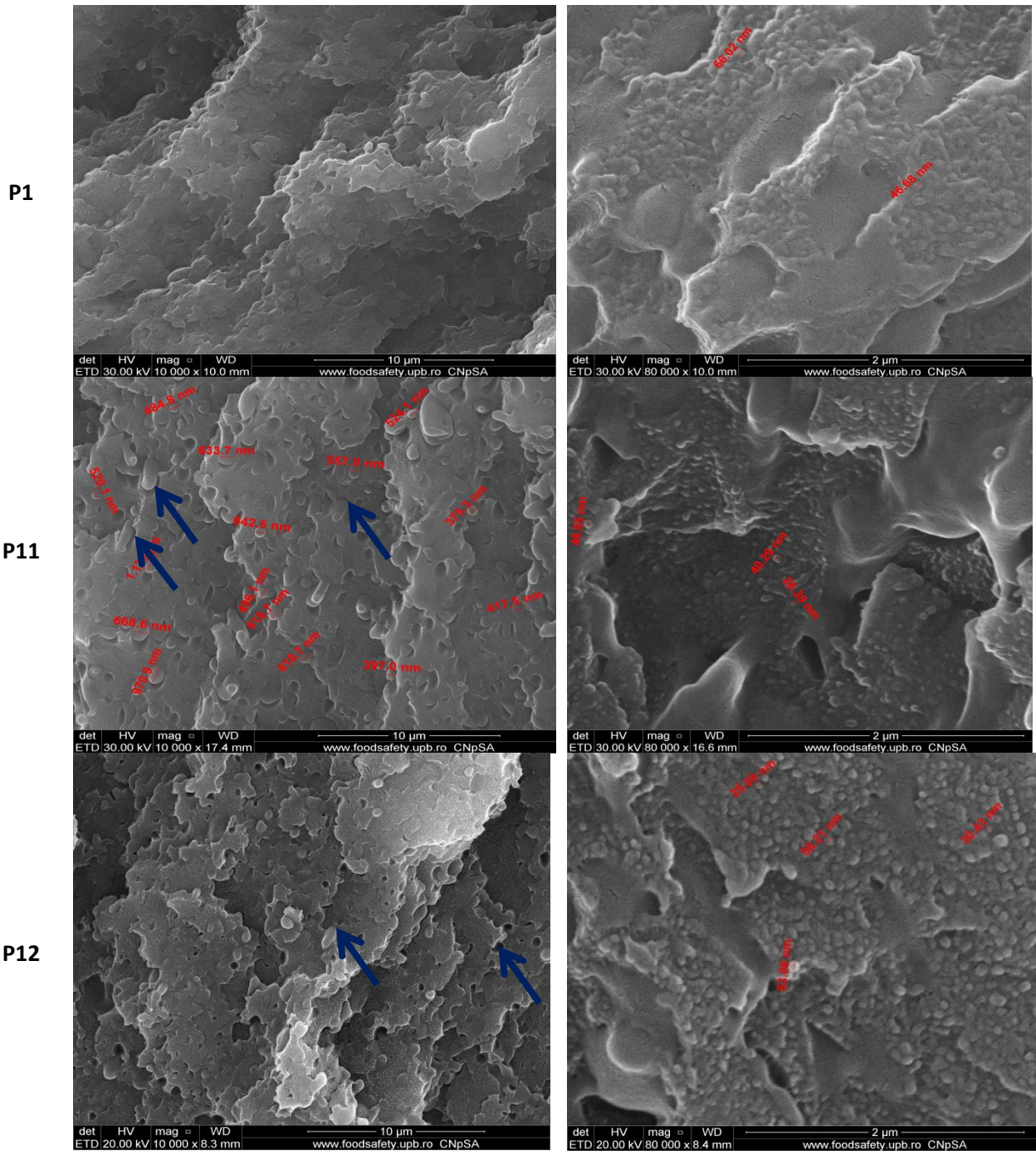


The SEM microscopies recorded for the P1 mixture and the P11-P14 composites were tested in the fracture section, resulted after Charpy resistance determination. As shown in Figure 8, for all the blends / composites obtained, the degree of dispersion of PE-*g*-MA and the untreated / treated fibers is relatively homogeneous. No areas with poor or fibrous agglomeration areas could be seen in PE-*g*-MA. In the case of the P1 mixture, a very good dispersion of PE-*g*-MA in the PETr mass (in the form of spherical particles with dimensions between 46-66 nm) is observed. As a result of the material failure, no voids could be seen, due to a high interaction between the polymeric phases. This demonstrates that PE-*g*-MA improves PETr ductility and adsorbs much of the applied energy. In the case of the P11 mixture, a good dispersion of untreated fibers in the mass of polymers, and the

deposition of a substantial layer of polymer on the surface of the fibers can be observed. However, due to poor interactions, the adhesion between the matrix and the fiber is weak, and leads to the separation of the fibers, following the applied energy. In the case of the P12 mixture, a good coating of hemp fibers with polymers, as well as the presence of voids in the material due to fiber pulling, is observed, which shows a poor interaction between the components. However, the fibers remaining after the impact do not show the debonding phenomenon, as in the case of P11. In the case of P13 mixture, which contains TiO₂ modified hemp fibers, a very good adhesion between the phases is observed, and the fibers are virtually completely embedded in the polymer matrix. The failure of the composite takes place predominantly at the fiber / matrix interface and not by fracture the fibers or pulling out.

This behavior confirms with certainty the very good resistances obtained by bending and impact. In case of P14 mixture, hemp fibers can not be viewed, probably due to the deposition

of a more generous polymer layer on their surface, which confirms the very good shock resistance of the hemp.



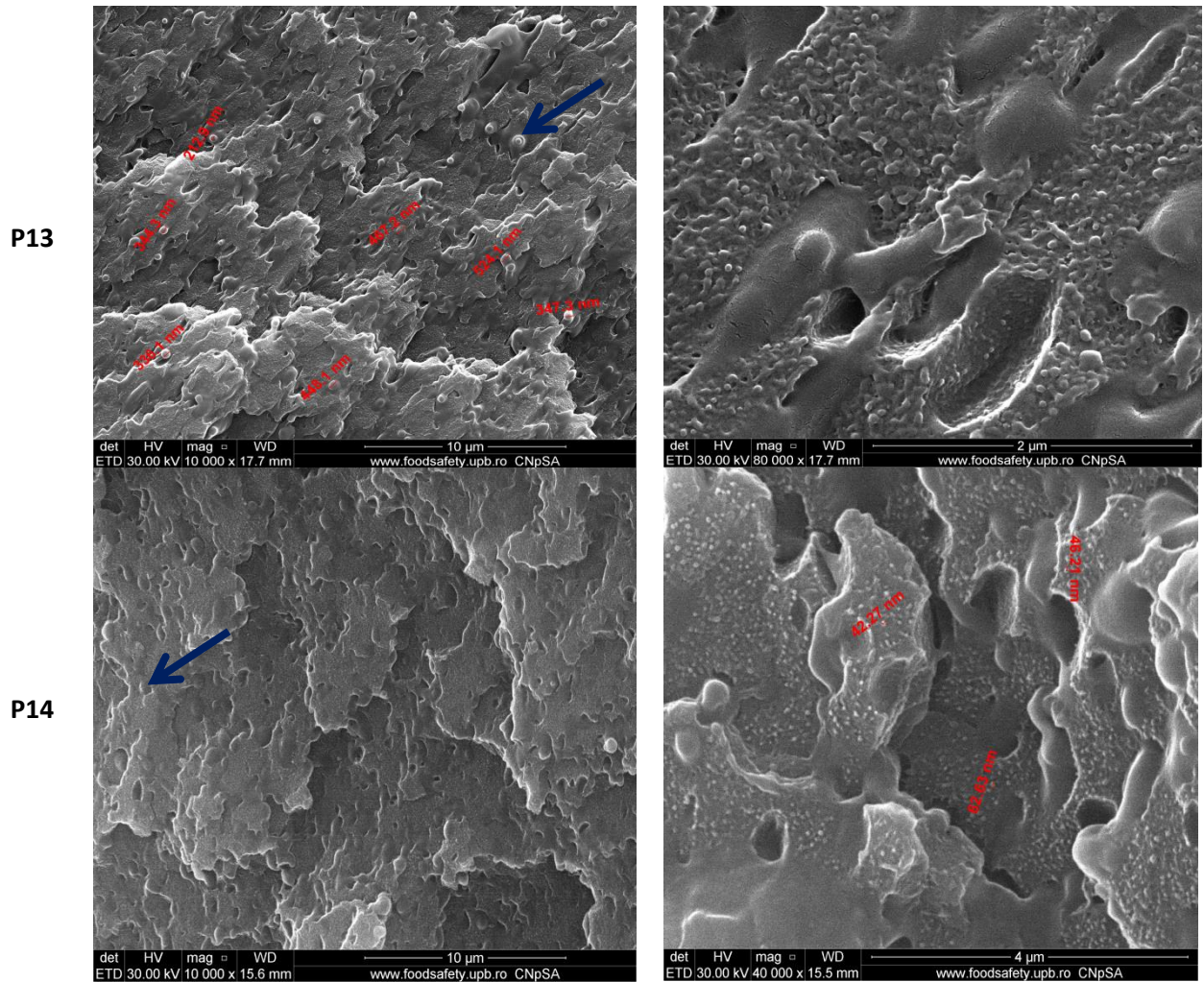


Figure 8. SEM images for P1, P11-P14 samples, at various magnifications, 10000, 80000 and/or 40000x

EDS analysis is a useful method of identifying the constituent elements existing in a sample. In this case, EDS analysis was performed to identify the distribution of TiO_2 from P13 and P14 samples containing TiO_2 as a consequence of the functionalization of the

hemp fibres with 1 and 5% titanium isopropoxide. As can be seen from Figure 9, the presence of Ti, could be identified in the sample, but in a small amount, if we relate to the relative intensity of C.

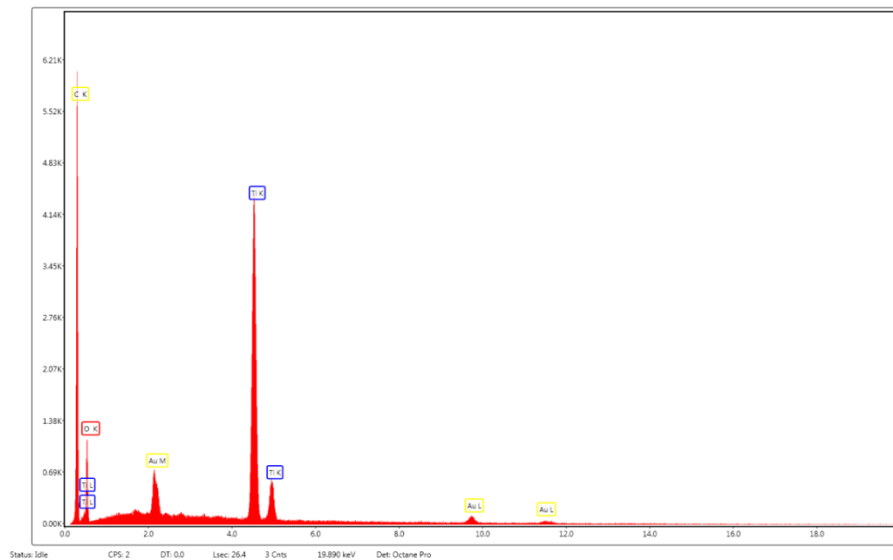


Figure 9. EDS spectra for P13 samples

The EDS spectra of sample P14 shown in Figure 10 highlights a substantial amount of TiO_2 present at the failure surface which can be explained based on the higher amount of TiO_2 deposited onto the surface of the hemp fibres. Also, combining EDS data with the SEM data it can conclude that SEM images of P14 do not

reveal any fibres extremity at the fracture surface which could be explained if accepting that over certain content of TiO_2 the detaching appear at the TiO_2 layer allowing in fact the pulling out of the hemp fibres partially coated with TiO_2 while another part remain at the PET mass.

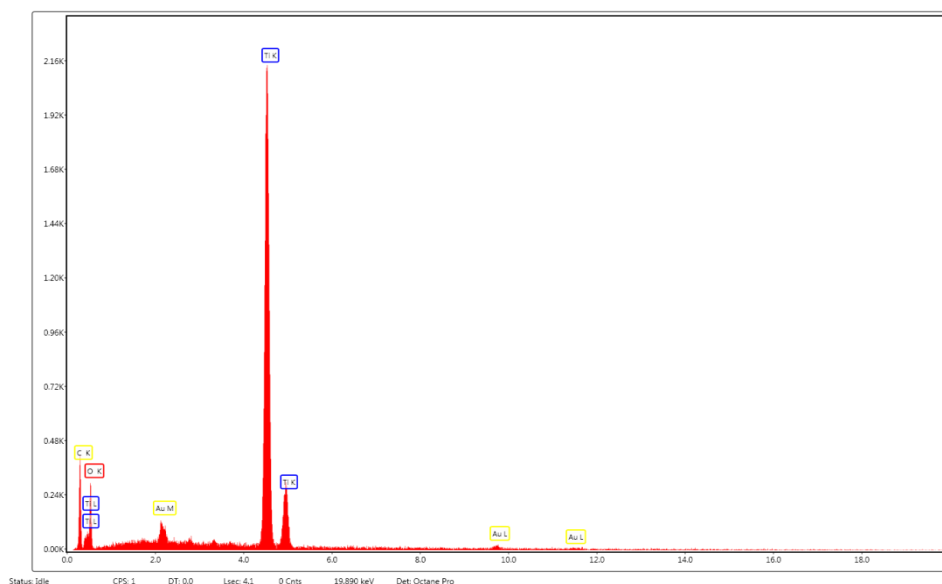


Figure 10. EDS spectra for P14 sample

FTIR Microscopy

The reference as well as the short fibers reinforced composite materials were analysed by FTIR and found similar spectra (Figure 11). All the spectra were overlaid such as the most intense peak appearing at 724cm^{-1} to have the same intensity for all the spectra. The

reference sample (P1) containing only PET and PE-g-MA can be considered a first reference sample and comparing with the P11 which additionally contains 4% hemp fibres, a strong water adsorption as well as the splitting of the band from 1092cm^{-1} can be seen. According to FTIR database the main peaks of PET appears at 1721, 1270, 1129, 1107, 1020, 872 and

728 cm^{-1} while the main peaks of hemp fibres appear at 2917, 2850, 1734, 1426, 1368, 1315, 1202, 1159, 1107, 1055, 1030, 897, 704 cm^{-1} . Also, for all the samples, the intensity of the bands corresponding to CH_2 decreased significantly as a consequence of the functionalization, the samples obtained with functionalized hemp fibres (P13 and P14) exhibiting the lowest peaks at about 2850 and 2920 cm^{-1} being shielded by the TiO_2 layer.

Based on these data, the distribution of the components is highlighted in Figures 11-16 at 1130 cm^{-1} (strong peak corresponding to PET), 1265 cm^{-1} (strong peak corresponding to hemp fibres) and 3430 cm^{-1} free OH groups. Based on the analysis of the spectra, it can be seen that only the peaks of PET and PE-g-MA appear which means that hemp fibres are well covered by the polymeric blend.

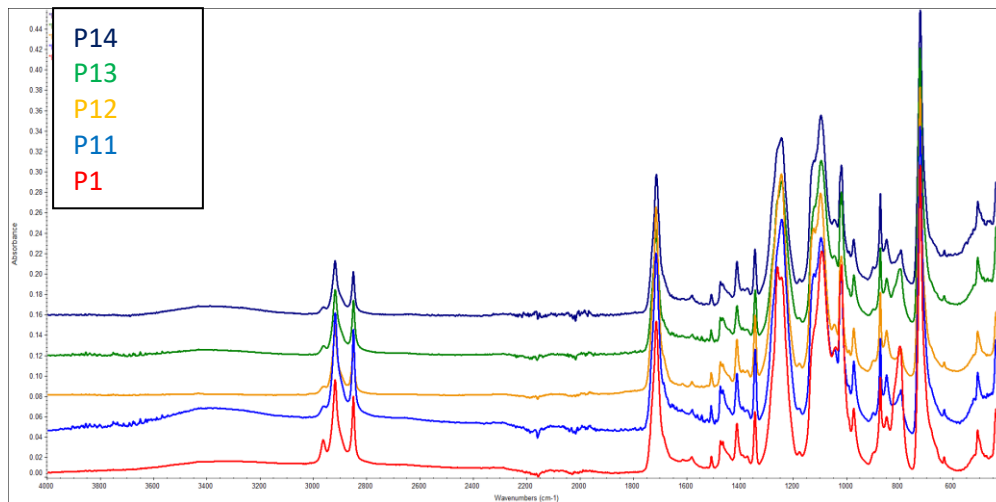


Figure 11. FTIR spectra of the reference / short fibres reinforced composite materials

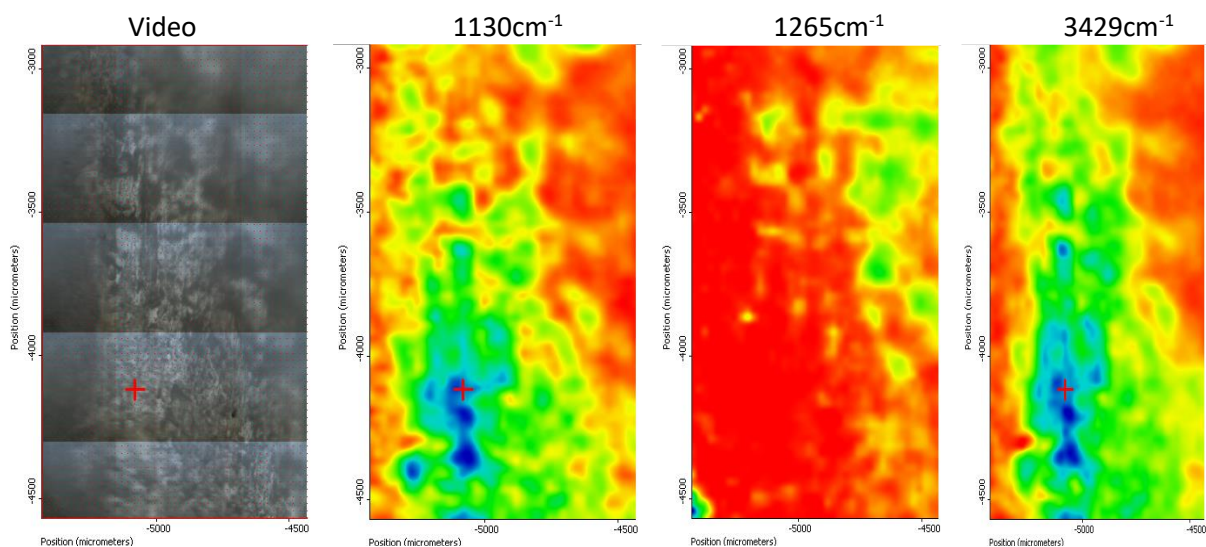


Figure 12. FTIR and video image of the P1 mixture (PETr/30%PE-g-MA)

In microscopy, certain important differences can be highlighted. In the case of P11 (Figure 13), it can be observed that all the components are homogeneously distributed which means that water absorption mainly occurs at the level of hemp fibres. The distribution of the short fibres within the composite materials is very good, in fact there

are no significant heterogeneities (very good similarity between the four representative maps recorded at 1130, 1265, 3429 and 2850 cm^{-1}). The same conclusion was obtained for the sample P12, Figure 14, obtained in similar conditions with P11 but maintaining hemp fibres in isopropanol before drying and use for obtaining the composite materials.

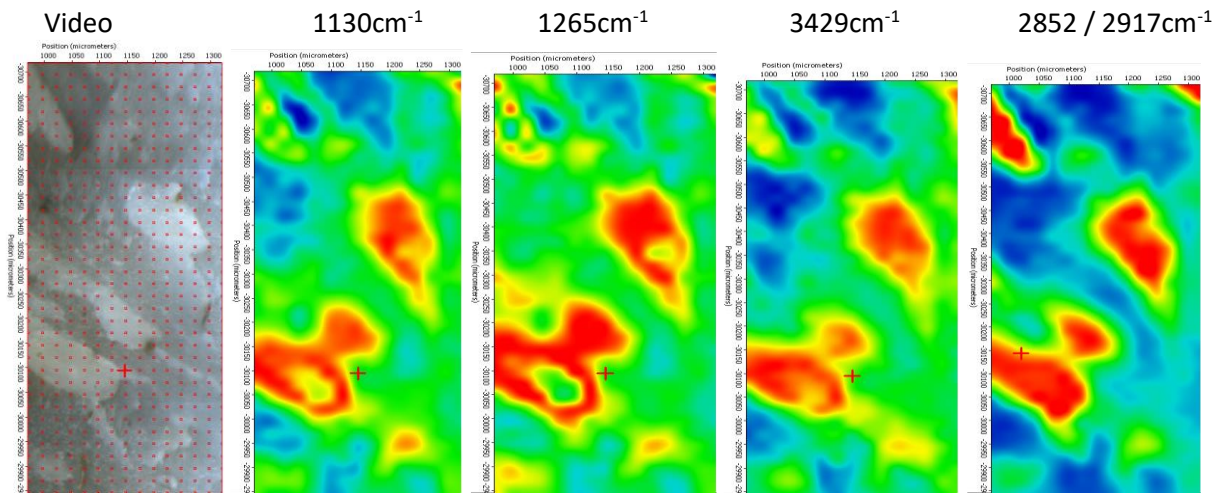


Figure 13. FTIR and video images of P11 sample (PETr/30%PE-g-MA/ Untreated hemp fibers)

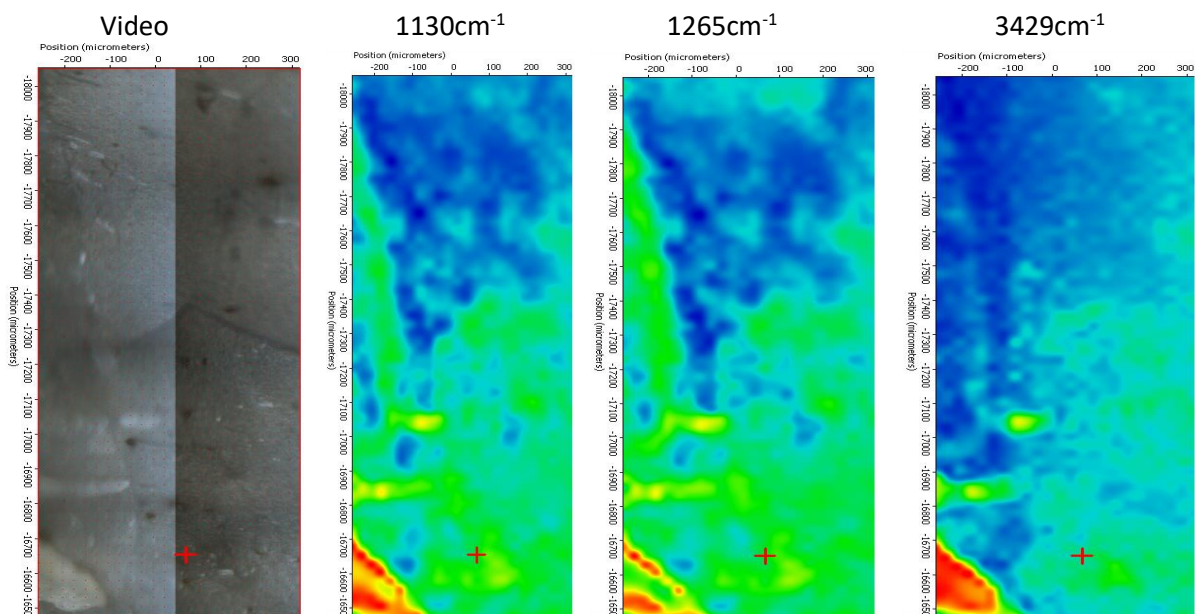


Figure 14. FTIR and video images of P12 sample (PETr/30%PE-g-MA/ Hemp fibers immersed in isopropanol)

When functionalised hemp fibres are used, some important changes appear. First of all, the peaks of hemp as well as the peaks corresponding to adsorbed water decreases because of the presence of TiO_2 nanoparticles which cover the hemp fibres. Also, because of the surface modification of the hemp fibres, the peaks corresponding to CH_2 decrease because they are shielded by the oxide layer. Two spectra corresponding to two different areas of the samples, marked with 1 and 2 are presented below, Figure 15, and based on

these spectra the FTIR maps are presented in Figure 16. Based on these spectra as well as on the different distribution of the main peaks it can be concluded that a heterogeneous structure is obtained because of the heterogeneous fracture through the material. Similar results are obtained also for the P14 samples, Figure 17 but in this case, the differences between the maps recorded at the three selected wavelengths are much more evident because the fracture is preferential.

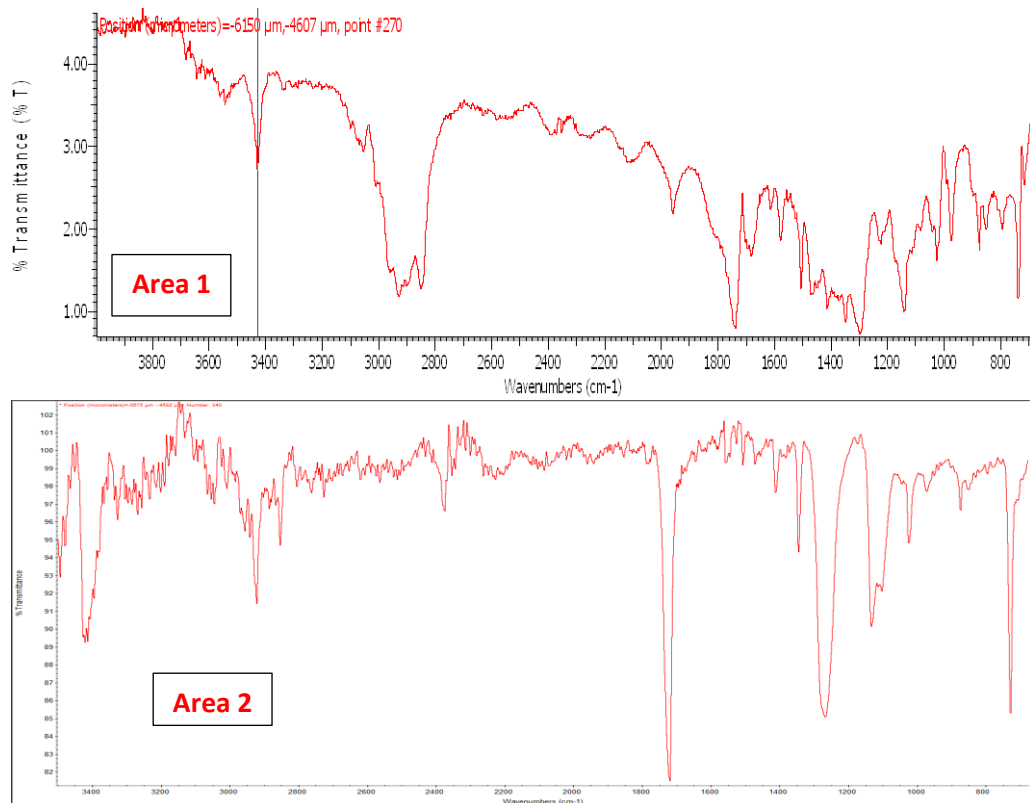


Figure 15. The FTIR spectra of the P13 sample recorded in the 1 and 2 area (PETr/30%PE-g-MA/4% hemp fibres/1% titanium isopropoxide)

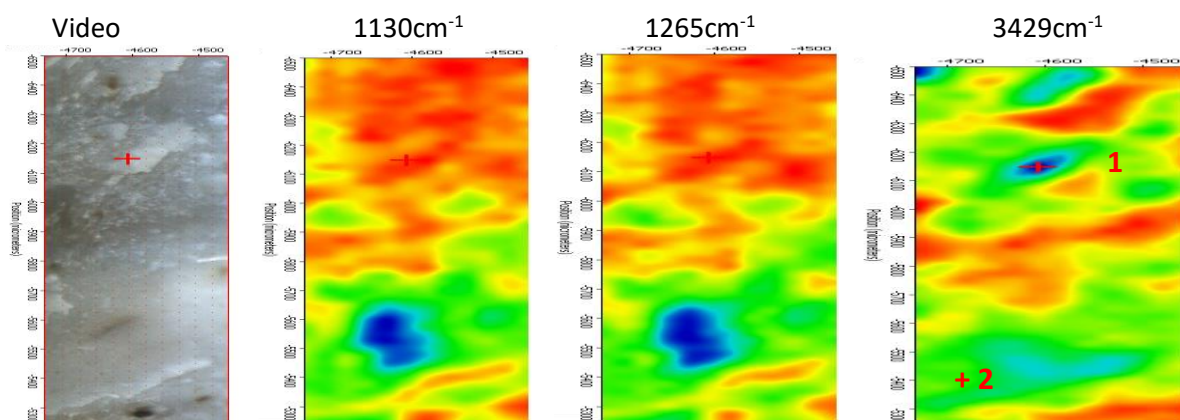


Figure 16. FTIR and video images of P13 sample

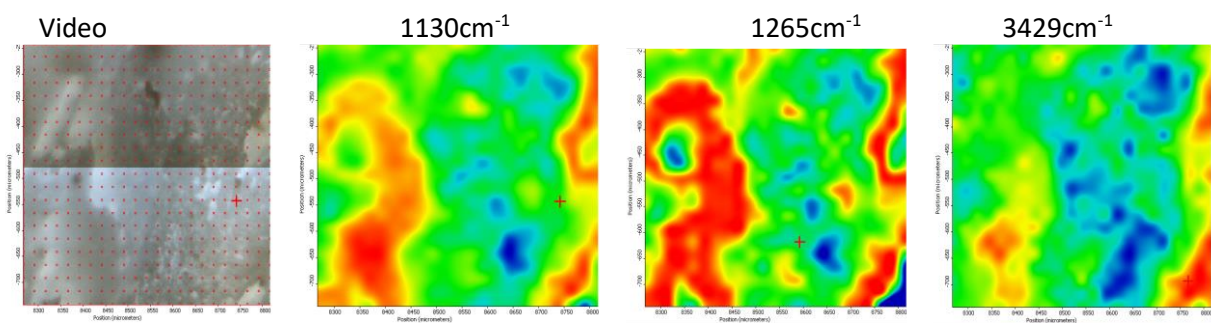


Figure 17. FTIR and video images of P14 sample (PETr/30%PE-g-MA/4% hemp fibres/5% titanium isopropoxide)

CONCLUSIONS

The main objective of the paper was to study the effect of the addition of compatibilizer – PE-*g*-MA and untreated / treated hemp fibers on the mechanical, morphological and rheological properties of PETr. Also, the use of PE-*g*-MA, can limit the thermo-oxidative degradation processes to which PETr is subjected during reprocessing. The formation of bonds between the polyester terminal groups and the PE-*g*-MA anhydride groups increases the viscosity of the mixture and, implicitly, the molecular weight. These findings are supported by the torque values obtained with PETr / PE-*g*-MA (P1), which are clearly superior to those recorded for PETr. It was found that if non-functionalized hemp fiber or only immersed in isopropanol is introduced into the PETr / PE-*g*-MA mix, the torque decreases compared to the one obtained for the P1 sample but increases compared to that obtained for PETr, due to poor interactions between components. Instead, the addition of modified hemp fibers with 1 or 5% TiO₂ improves the torque value to close to that obtained for the P1 sample. Mechanical properties (flexural, modulus, elongation, shock) are greatly improved by simply adding PE-*g*-MA to PETr, due to the reduction of PETr fragility. However, the Vicat temperature is clearly below PETr. In the case of composites containing untreated fibers, mechanical properties are reduced due to poor interface interactions. The best mechanical properties were obtained in the case of adding functionalized fibers, due to very strong interactions developed at the interface. SEM and FTIR microscopy confirm a good coverage of the fibers with polymer, a very good dispersion of both PE-*g*-MA and PETr mass. In the case of composites containing untreated fibers, the main material failure mechanism is by debonding and pulling out. Instead, in the case of treated fibers, due to a very good interface between the components (the fibers are fully embedded in the matrix), failure occurs exclusively by fibers fracture to the interface. Areas associated with fiber pullouts cannot be viewed. FTIR spectra and FTIR microscopy confirm a very good polymer

coating of fibers. Based on the results, it can be concluded that the PETr processing by the addition of suitable components leads to the achievement of some high-performance properties and offers the premises for the use of these low-cost materials in various applications in automotive, construction industry, etc. Moreover, these materials can successfully replace conventional composites, based on virgin polymers, reinforced with synthetic fibers in various applications, with some more environmentally friendly, more cost-effective (due to the abundance and the lower price of recycled polymers and natural fibers) materials, and with a lower impact on human health.

Acknowledgements

This research was financed through PN-III-P2-2.1-PTE-2016 project: Recovery of Recycled Thermoplastic Polymers by Reinforcement with Functionalized Natural Fibres to Obtain New Added Value Products, contract no. 20 PTE/2016, supported by MECS-UEFISCDI.

REFERENCES

1. Lima, P.S., Brito, R.S.F., Santos, B.F.F., Tavares, A.A., Agrawal, P., Andrade, D.L.A.C.S., Wellen, R.M.R., Canedo, E.L., Silva, S.M.L., Rheological Properties of HDPE/Chitosan Composites Modified with PE-*g*-MA, *J Mater Res*, **2017**, 32, 775-787, <https://doi.org/10.1557/jmr.2016.519>.
2. Leão, R.M., da Luz, M.S., Araújo, J.A., Christoforo, A.L., The Recycling of Sugarcane Fiber/Polypropylene Composites, *Mater Res*, **2015**, 18, 4, 690-697, <https://doi.org/10.1590/1516-1439.321314>.
3. Lu, N., Swan, R.H. Jr., Ferguson, I., Composition, Structure, and Mechanical Properties of Hemp Fiber Reinforced Composite with Recycled High-Density Polyethylene Matrix, *J Compos Mater*, **2012**, 46, 1915–1924, <https://doi.org/10.1177/0021998311427778>.
4. Tran, L.Q.N., Yuan, X., Bhattacharyya, D., Fuentes, C.A., Van Vuure, A.W., Verpoest, I., Fiber-matrix Interfacial Adhesion in Natural Fiber Composites, *Int J Modern Phys B*, **2015**, 29, 10n11, 1540018, <https://doi.org/10.1142/S0217979215400184>.
5. Yang, X., Wang, G., Miao, M., Yue, J., Hao, J., Wang, W., The Dispersion of Pulp-Fiber in High-Density Polyethylene via Different Fabrication

- Processes, *Polymers*, **2018**, 10, 2, 122, <https://doi.org/10.3390/polym10020122>.
6. Zaki Abdullah, M., Dan-mallam, Y., Megat-Yusoff, P.S.M., Effect of Environmental Degradation on Mechanical Properties of Kenaf/Polyethylene Terephthalate Fiber Reinforced Polyoxymethylene Hybrid Composite, *Adv Mater Sci Eng*, **2013**, 671481, <https://doi.org/10.1155/2013/671481>.
 7. Ahmad, M.A.A., Majid, M.S.A., Ridzuan, M.J.M., Firdaus, A.Z.A., Amin, N.A.M., Tensile Properties of Interwoven Hemp/PET (Polyethylene Terephthalate) Epoxy Hybrid Composites, *J Phys Conf Ser*, **2017**, 908, 012011, <https://doi.org/10.1088/1742-6596/908/1/012011>.
 8. Owen, M.M., Ishiaku, U.S., Danladi, A., Dauda, B.M., Romli, A.Z., The Effect of Surface Coating and Fibre Loading on Thermo-Mechanical Properties of Recycled Polyethylene Terephthalate (RPET)/Epoxy-Coated Kenaf Fibre Composites, *National Symposium on Polymeric Materials*, **2018**, 1985, 1, <https://doi.org/10.1063/1.5047160>.
 9. Holbery, J., Houston, D., Natural-Fiber-Reinforced Polymer Composites in Automotive Applications, *JOM*, **2006**, 58, 80-86, <https://doi.org/10.1007/s11837-006-0234-2>.
 10. Dhakal, H.N., Sarasini, F., Santulli, C., Tirillò, J., Zhang, Z., Arumugam, V., Effect of Basalt Fibre Hybridisation on Post-Impact Mechanical Behaviour of Hemp Fibre Reinforced Composites, *Compos A Appl Sci Manuf*, **2015**, 75, 54-67, <https://doi.org/10.1016/j.compositesa.2015.04.020>.
 11. Merdan, N., Effects of Environmental Surface Modification Methods on Physical Properties of Hemp Fibers, *Materials Science*, **2017**, 23, 416-421, <https://doi.org/10.5755/j01.ms.23.4.17469>.
 12. Karaduman, Y., Ozdemir, H., Karaduman, N.S., Ozdemir, G., Interfacial Modification of Hemp Fiber-Reinforced Composites, in: E. Günay (ed.), *Natural and Artificial Fiber-Reinforced Composites as Renewable Sources*, IntechOpen, **2018**, 17-39, <https://doi.org/10.5772/intechopen.70519>.
 13. Kumar, R., Obrai, S., Sharma, A., Chemical Modifications of Natural Fiber for Composite Material, *Der Chemica Sinica*, **2011**, 2, 4, 219-228.
 14. Regazzi, A., Corn, S., Ienny, P., Bergeret, A., Coupled Hydro-Mechanical Aging of Short Flax Fiber Reinforced Composites, *Polym Degrad Stab*, **2016**, 130, 300-306, <https://doi.org/10.1016/j.polymdegradstab.2016.06.016>.
 15. Naidu, A.L., Raghuveer, D., Suman, P., Studies on Characterization and Mechanical Behavior of Banana Peel Reinforced Epoxy Composites, *Int J Sci Eng Res*, **2013**, 4, 6, 844-851.
 16. Pickering, K.L., Aruan Efendy, M.G., Le, T.M., A Review of Recent Developments in Natural Fibre Composites and Their Mechanical Performance, *Compos A Appl Sci Manuf*, **2016**, 83, 98-112, <https://doi.org/10.1016/j.compositesa.2015.08.038>.
 17. Rohit, K., Dixit, S., A Review - Future Aspect of Natural Fiber Reinforced Composite, *Polym Renew Resour*, **2016**, 7, 43-60, <https://doi.org/10.1177/204124791600700202>.
 18. Talla, A.S.F., Erchiqui, F., Kaddami, H., Kocafee, D., Investigation of the Thermostability of Poly(ethylene Terephthalate)-Hemp Fiber Composites: Extending Natural Fiber Reinforcements To High-Melting Thermoplastics, *J Appl Polym Sci*, **2015**, 1-10, <https://doi.org/10.1002/app.42500>.
 19. Fotso Talla, A.S., Erchiqui, F., Godard, F., Thermal Properties and Stability of PET-Hemp Fibers Composites, The 19th International Conference on Composite Materials (ICCM'19), **2013**, Montreal, Canada.
 20. Shahzad, A., Hemp Fiber and Its Composites – A Review, *J Compos Mater*, **2012**, 46, 973-986, <https://doi.org/10.1177/0021998311413623>.
 21. Ngo, T.D., Natural Fibers for Sustainable Bio-Composites, in: E. Günay (ed.), *Natural and Artificial Fiber-Reinforced Composites as Renewable Sources*, IntechOpen, **2018**, <https://doi.org/10.5772/intechopen.71012>.
 22. Awaja, F., Pavel, D., Statistical Models for Optimisation of Properties of Bottles Produced Using Blends of Reactive Extruded Recycled PET and Virgin PET, *Eur Polym J*, **2005**, 41, 2097-2106, <https://doi.org/10.1016/j.eurpolymj.2005.04.010>.
 23. Alaerts, L., Augustinus, M., Van Acker, K., Impact of Bio-Based Plastics on Current Recycling of Plastics, *Sustainability*, **2018**, 10, 1-15, <https://doi.org/10.3390/su10051487>.
 24. Tan, C., Ahmad, I., Heng, M., Characterization of Polyester Composites from Recycled Polyethylene Terephthalate Reinforced with Empty Fruit Bunch Fibers, *Mater Des*, **2011**, 32, 4493-4501, <https://doi.org/10.1016/j.matdes.2011.03.037>.
 25. Khoramnejadian, S., Improve Properties of Recycled Poly Ethylene Terephthalat (PET) By Polycarbonate, *Asian J Research Chem*, **2011**, 4, 10, 1539-1541.
 26. Lima, A.C., Monteiro, S.N., Satyanarayana, K.G., Recycled Polyethylene Composites Reinforced with Jute Fabric from Sackcloth: Part II-Impact Strength Evaluation, *J Polym Environ*, **2011**, 19,

- 957–965, <https://doi.org/10.1007/s10924-011-0347-8>.
27. Chiu, H.T., Hsiao, Y.K., Compatibilization of Poly(ethylene terephthalate)/Polypropylene Blends with Maleic Anhydride Grafted Polyethylene-Octene Elastomer, *J Polym Res*, **2006**, 13, 153–160, <https://doi.org/10.1007/s10965-005-9020-z>.
 28. Tajvidi, M., Motie, N., Mechanical Performance of Hemp Fiber Polypropylene Composites at Different Operating Temperatures, *J Reinf Plast Compos*, **2010**, 29, 664-674, <https://doi.org/10.1177/0731684408100266>.
 29. Cicala, G., Tosto, C., Latteri, A., La Rosa, A.D., Blanco, I., Elsabbagh, A., Russo, P., Ziegmann, G., Green Composites Based on Blends of Polypropylene with Liquid Wood Reinforced with Hemp Fibers: Thermomechanical Properties and the Effect of Recycling Cycles, *Materials*, **2017**, 10, 1-16, <https://doi.org/10.3390/ma10090998>.
 30. Fortea-Verdejo, M., Bumbaris, E., Burgstaller, C., Bismarck, A., Lee, K.Y., Plant Fibre-Reinforced Polymers: Where Do We Stand in Terms of Tensile Properties?, *Int Mater Rev*, **2017**, 62, 441-464, <https://doi.org/10.1080/09506608.2016.1271089>.
 31. Duarte, I.S., Tavares, A.A., Lima, P.S., Andrade, D.L.A.C.S., Carvalho, L.H., Canedo, E.L., Silva, S.M.L., Chain Extension of Virgin and Recycled Poly(ethylene Terephthalate): Effect of Processing Conditions and Reprocessing, *Polym Degrad Stab*, **2016**, 124, 26-34, <https://doi.org/10.1016/j.polymdegradstab.2015.11.021>.
 32. Tavares, A.A., Silva, D.F.A., Lima, P.S., Andrade, D.L.A.C.S., Silva, S.M.L., Canedo, E.L., Chain Extension of Virgin and Recycled Poly(ethylene Terephthalate): Effect of Processing Conditions and Reprocessing, *Polym Test*, **2016**, 50, 26-32, <https://doi.org/10.1016/j.polymertesting.2015.11.020>.
 33. Lei, Y., Wu, Q., Clemons, C.M., Guo, W., Phase Structure and Properties of Poly(ethylene Terephthalate)/High-Density Polyethylene Based on Recycled Materials, *J Appl Polym Sci*, **2009**, 113, 1710-1719, <https://doi.org/10.1002/app.30178>.
 34. Pereira, L.M., Corrêa, A.C., De Souza Filho, M.M., De Freitas Rosa, M., Itod, E.N., Rheological, Morphological and Mechanical Characterization of Recycled Poly (ethylene Terephthalate) Blends and Composites, *Mater Res*, **2017**, 20, 791-800, <https://doi.org/10.1590/1980-5373-mr-2016-0870>.
 35. İzgi, A.A., Koçak, E.D., Yılmaz Şahinbaşkan, B., Merdan, N., Ardiç, B., Studies on Mechanical Performance of *Cynara scolymus*/Polyethylene Terephthalate Nonwoven Composites, *Selçuk-Teknik Dergisi*, **2018**, 107-116.
 36. Ahmad, M.A.A., Abdul Majid, M.S., Ridzuan, M.J.M., Mazlee, M.N., Gibson, A.G., Dynamic Mechanical Analysis and Effects of Moisture on Mechanical Properties of Interwoven Hemp/Polyethylene Terephthalate (PET) Hybrid Composites, *Constr Build Mater*, **2018**, 179, 265-276, <https://doi.org/10.1016/j.conbuildmat.2018.05.227>.
 37. Alavudeen, A., Rajini, N., Karthikeyan, S., Thiruchitrabalam, M., Venkateshwaren, N., Mechanical Properties of Banana/Kenaf Fiber-Reinforced Hybrid Polyester Composites: Effect of Woven Fabric and Random Orientation, *Mater Des*, **2015**, 66, 246-257, <https://doi.org/10.1016/j.matdes.2014.10.067>.
 38. Gallos, A., Paes, G., Allais, F., Beaugrand, J., Lignocellulosic Fibers: A Critical Review of the Extrusion Process for Enhancement of the Properties of Natural Fiber Composites, *RSC Adv*, **2017**, 7, 34638–34654, <https://doi.org/10.1039/C7RA05240E>.
 39. Srinivas, K., Lakshumu Naidu, A., Raju Bahubalendruni, M.V.A., A Review on Chemical and Mechanical Properties of Natural Fiber Reinforced Polymer Composites, *Int J Perform Eng*, **2017**, 13, 189-200.
 40. Guessoum, M., Medjdoub, N., Nekkaa, S., Haddaoui, N., Rheological and Mechanical Properties of Recycled Poly(ethylene Terephthalate)/High Density Polyethylene Blends, *MATEC Web of Conferences*, Vol. 5, 04026, **2013**, <https://doi.org/10.1051/mateconf/20130504026>.
 41. Liping, H., Li, W., Chen, D., Zhou, D., Lu, G., Yuan, J., Effects of Amino Silicone Oil Modification on Properties of Ramie Fiber and Ramie Fiber/Polypropylene Composites, *Mater Des*, **2015**, 77, 142-148, <https://doi.org/10.1016/j.matdes.2015.03.051>.
 42. Zimmermann, M.V.G., Zattera, A.J., Recycling and Reuse of Waste from Electricity Distribution Networks as Reinforcement Agents in Polymeric Composites, *Waste Manage*, **2013**, 33, 7, 1667-1674, <https://doi.org/10.1016/j.wasman.2013.04.002>.
 43. Abu Bakar, A., Hariharan, H.P.S., Khalil, A., Lignocellulose-based Hybrid Bilayer Laminate Composite: Part I - Studies on Tensile and Impact Behavior of Oil Palm Fiber-Glass Fiber-reinforced Epoxy Resin, *J Compos Mater*, **2005**, 39, 663-684, <https://doi.org/10.1177/0021998305047267>.
 44. Zhang, H., Zhang, Y., Guo, W., Xu, D., Wu, C., Thermal Properties and Morphology of Recycled Poly(ethylene Terephthalate)/Maleic Anhydride Grafted Linear Low-density Polyethylene

Blends, *J Appl Polym Sci*, **2008**, 109, 3546-3553,
<https://doi.org/10.1002/app.28456>.
45. Dan-mallam, Y., Abdullah, M.Z., Puteri Sri Yusoff,
M.M., Mechanical Properties of Recycled

Kenaf/Polyethylene Terephthalate (PET) Fiber
Reinforced Polyoxymethylene (POM) Hybrid
Composite, *J Appl Polym Sci*, **2014**,
<https://doi.org/10.1002/app.39831>.

© 2024 by the author(s). Published by INCDTP-ICPI, Bucharest, RO. This is an open access article distributed under the terms and conditions of the Creative Commons Attribution license (<http://creativecommons.org/licenses/by/4.0/>).